Observer design for bilateral teleoperators with variable time delays

Laura López–Recillas * **Mauro López** * **Emmanuel Nuño** **

* *Departamento de Control y Robótica, División de Ingeniería Eléctrica de la Facultad de Ingeniería. Universidad Nacional Autónoma de México. Apdo. Postal 70–256, México, CDMX, 04510, México. Email: marteagp@unam.mx.*
** *Departamento de Ciencias Computacionales, Centro Universitario de Ciencias Exactas e Ingenierías, Universidad de Guadalajara. Guadalajara, Mexico. Email: emmanuel.nuno@cucei.udg.mx*

Abstract: This paper addresses the control–observer design problem for bilateral teleoperation systems that employ communication channels that impose variable time delays. These delays are a function of different factors such as, for example, congestion, bandwidth or distance. Teleoperation systems allow people to perform complex tasks in remote or inaccessible environments. However, due to time delays, performance is downgraded because exact position tracking and transparency cannot be simultaneously achieved. For this reason, most control approaches are meant to guarantee only position regulation and most algorithms are designed assuming that joint velocity measurements are available. The control–observer scheme proposed in this paper does not make use of velocity measurements and, more importantly, does not require the exact knowledge of the dynamical model. It is shown that the velocity observation errors tend to zero while position tracking is achieved in free motion. Additionally, in constrained motion, the human operator has force feedback and therefore his/her feeling of telepresence is increased. Particular emphasis is shown in the experimental results, which validate the proposed control algorithm.

Keywords: Bilateral teleoperators, observer design, variable time delays.

1. INTRODUCTION

Bilateral local–remote teleoperation systems allow people to perform complex tasks in environments that are not accessible, because of their remoteness or the presence of hazards. These systems combine human skills, such as reasoning and decision making, with the advantages of robotic manipulation. A teleoperation system is composed of five essential elements: the human operator, the local robot, the communication channel, the remote robot and the environment. Ideally, telepresence, task performance, and transparency are simultaneously optimized without risking the stability of the closed–loop system (Passenberg et al., 2010). Task performance and robustness are required features while telepresence and transparency are ideal goals (Nuño et al., 2011). Otherwise, the mechanism cannot be intuitively used and the operator would have to be specially trained. The first two features have been extensively studied while the other two are challenges for real–time applications (Hokayem and Spong, 2006).

Some of the capabilities of bilateral teleoperation systems rely in the exchange of measurements of positions, velocities and forces through a communication channel. However, these communications can induce substantial delays between the command given by the human operator and the moment this command is received by the remote robot. Furthermore, the information that is sent back endures also a time-delay (Nuño et al., 2008, 2009). Due to the presence of time-delays, exact tracking position and perfect transparency cannot be simultaneously achieved. For this reason, most control approaches are meant to guarantee only position regulation. The consensus problem is a more challenging goal, where two or more manipulators tend to reach a particular position, both in the presence and in the absence of a leader (Aldana et al., 2015). Also, another particular objective may be the synchronization of a set of robots by inducing periodic position trajectories (Chopra et al., 2008).

Most control algorithms are designed assuming that joint velocities are available. To overcome this difficulty, in (Sarras et al., 2016) the Immersion and Invariance (I&I) velocity observer (Astolfi et al., 2010) has been ported to the bilateral teleoperation control. However, for the observer design, in such a case it is necessary to have an exact knowledge of the complete system dynamics. In (Arteaga-Pérez et al., 2016) a control–observer scheme is proposed that guarantees that position and observation errors can be made arbitrarily small with a proper gain tuning without requiring the exact knowledge of the system dynamics. However, only constant time-delays are considered. Another recent work that deals with a similar problem is (Nuño and Ortega, 2017) where the energy shaping methodology has been extended to deal with the consensus of networks of robots with interconnection delays. The controller proposed by Nuño and Ortega (2017) does not rely on velocity measurements. However, the dynamic controller that they propose can be seen as a second order velocity filter and not a velocity observer.

In this paper, following the previous work of (Arteaga-Pérez et al., 2017), the scheme introduced in (Arteaga-Pérez et al., 2016) is modified to deal with variable time-delays. Furthermore, observation errors are observed to tend to zero (and not only to be ultimately bounded) while position errors can be made arbitrarily small in free movement or become zero when the human does not interact with the local robot. In the case when a human operator moves one of the robots, the other follows the commanded (delayed) trajectory. The work of (Arteaga-Pérez et al., 2017) assumes that the human operator behaves as a PD controller. In this work, an experimental validation of the proposed control algorithm is shown and therefore, there is not any assumption regarding the human operator behavior.

The rest of the paper is organized as follows. The local and remote robot models, as well as some properties are given in Section 2. The control–observer scheme is proposed in Section 3. Section 4 presents some experimental results. The paper conclusions are stated in Section 5.

2. DYNAMIC MODEL OF A TELEOPERATOR

Consider a local (l)–remote (r) robot teleoperation system composed of two manipulators. Each of them with n–degrees of freedom, but not necessarily with the same kinematic configuration. The local dynamics is given by (Sarras et al., 2014):

$$\boldsymbol{H}_{\mathrm{l}}(\boldsymbol{q}_{\mathrm{l}})\ddot{\boldsymbol{q}}_{\mathrm{l}} + \boldsymbol{C}_{\mathrm{l}}(\boldsymbol{q}_{\mathrm{l}}, \dot{\boldsymbol{q}}_{\mathrm{l}})\dot{\boldsymbol{q}}_{\mathrm{l}} + \boldsymbol{D}_{\mathrm{l}}\dot{\boldsymbol{q}}_{\mathrm{l}} + \boldsymbol{g}_{\mathrm{l}}(\boldsymbol{q}_{\mathrm{l}}) = \boldsymbol{\tau}_{\mathrm{l}} - \boldsymbol{\tau}_{\mathrm{h}} \quad (1)$$

while the remote dynamics is modeled by:

$$\boldsymbol{H}_{\mathrm{r}}(\boldsymbol{q}_{\mathrm{r}})\ddot{\boldsymbol{q}}_{\mathrm{r}} + \boldsymbol{C}_{\mathrm{r}}(\boldsymbol{q}_{\mathrm{r}}, \dot{\boldsymbol{q}}_{\mathrm{r}})\dot{\boldsymbol{q}}_{\mathrm{r}} + \boldsymbol{D}_{\mathrm{r}}\dot{\boldsymbol{q}}_{\mathrm{r}} + \boldsymbol{g}_{\mathrm{r}}(\boldsymbol{q}_{\mathrm{r}}) = \boldsymbol{\tau}_{\mathrm{e}} - \boldsymbol{\tau}_{\mathrm{r}} \quad (2)$$

where for $i =$ l, r, $\boldsymbol{q}_i \in \mathbb{R}^n$ is the vector of generalized joint coordinates, $\boldsymbol{H}_i(\boldsymbol{q}_i) \in \mathbb{R}^{n\times n}$ is the symmetric positive definite inertia matrix, $\boldsymbol{C}_i(\boldsymbol{q}_i, \dot{\boldsymbol{q}}_i)\dot{\boldsymbol{q}}_i \in \mathbb{R}^n$ is the vector of Coriolis and centrifugal torques, $\boldsymbol{D}_i \in \mathbb{R}^{n\times n}$ is a diagonal positive semidefinite matrix accounting for viscous friction, $\boldsymbol{g}_i(\boldsymbol{q}_i) \in \mathbb{R}^n$ is the vector of gravitational torques and $\boldsymbol{\tau}_i \in \mathbb{R}^n$ is the vector of torques acting on the joints. $\boldsymbol{\tau}_{\mathrm{h}} \in \mathbb{R}^n$ represents the torque applied by the human to the local robot and $\boldsymbol{\tau}_{\mathrm{e}} \in \mathbb{R}^n$ the environment interaction.

Model (1) and (2) have the following properties (Kelly et al., 2005):

Property 1. It holds that $\lambda_{\mathrm{h}i}\|\boldsymbol{x}\|^2 \leq \boldsymbol{x}^\top \boldsymbol{H}_i(\boldsymbol{q}_i)\boldsymbol{x} \leq \lambda_{\mathrm{H}i}\|\boldsymbol{x}\|^2 \quad \forall\, \boldsymbol{q}_i, \boldsymbol{x} \in \mathbb{R}^n$, and $0 < \lambda_{\mathrm{h}i} \leq \lambda_{\mathrm{H}i} < \infty$, with $\lambda_{\mathrm{h}i} \stackrel{\triangle}{=} \lambda_{\min}(\boldsymbol{H}_i(\boldsymbol{q}_i))$ and $\lambda_{\mathrm{H}i} \stackrel{\triangle}{=} \lambda_{\max}(\boldsymbol{H}_i(\boldsymbol{q}_i))$. $\lambda_{\min}$ and $\lambda_{\max}$ denote the minimum and the maximum eigenvalue of a matrix, respectively. △

Property 2. With a proper definition of $\boldsymbol{C}_i(\boldsymbol{q}_i, \dot{\boldsymbol{q}}_i)$, $\dot{\boldsymbol{H}}_i(\boldsymbol{q}_i) - 2\boldsymbol{C}_i(\boldsymbol{q}_i, \dot{\boldsymbol{q}}_i)$ is skew symmetric. △

3. PROPOSED CONTROL–OBSERVER SCHEME

Suppose that there are time-delays imposed by the communication channel given by $T_{\mathrm{l}}(t) \geq 0$ and $T_{\mathrm{r}}(t) \geq 0$ and such delays satisfy the following assumption.

Assumption 1. The variable time-delay $T_i(t)$ has a known upper bound $\overline{T}_i$, *i. e.* $0 \leq T_i(t) \leq \overline{T}_i < \infty$, for $i =$l,r. Moreover, $\dot{T}_i(t)$ is bounded. △

3.1 Observer design

It is desired to design a position tracking control law while velocity measurements are not available. Assume for simplicity that the remote is in free movement, *i. e.* $\boldsymbol{\tau}_{\mathrm{e}} = \boldsymbol{0}$. Consider once again $i =$l, r, and define as desired trajectory

$$\boldsymbol{q}_{\mathrm{d}i} \stackrel{\triangle}{=} \boldsymbol{q}_j(t - T_j(t)), \quad (3)$$

where if $i =$ l, then $j =$ r and vice versa. Since $\dot{\boldsymbol{q}}_{\mathrm{d}i}$ is not available, consider the following definition

$$\boldsymbol{q}_{\mathrm{v}i} \stackrel{\triangle}{=} \dot{\hat{\boldsymbol{q}}}_j(t - T_j(t)), \quad (4)$$

where $(\hat{\cdot})$ is the estimated value of $(\cdot)$. Then, the corresponding observation and tracking errors are defined as

$$\boldsymbol{z}_i \stackrel{\triangle}{=} \boldsymbol{q}_i - \hat{\boldsymbol{q}}_i, \quad (5)$$

and

$$\Delta\boldsymbol{q}_i \stackrel{\triangle}{=} \boldsymbol{q}_i - \boldsymbol{q}_{\mathrm{d}i}, \quad (6)$$

respectively.

Based on (Arteaga-Pérez et al., 2006), we propose the following velocity observer

$$\dot{\boldsymbol{\xi}}_i = \boldsymbol{z}_i \quad (7)$$

$$\dot{\hat{\boldsymbol{q}}}_{\mathrm{o}i} = \boldsymbol{q}_{\mathrm{v}i} - \boldsymbol{\Lambda}_{\mathrm{x}i}\Delta\boldsymbol{q}_i + \boldsymbol{K}_{\mathrm{d}i}\boldsymbol{\Lambda}_{\mathrm{z}i}\boldsymbol{\xi}_i \quad (8)$$

$$\dot{\hat{\boldsymbol{q}}}_i = \dot{\hat{\boldsymbol{q}}}_{\mathrm{o}i} + \boldsymbol{\Lambda}_{\mathrm{z}i}\boldsymbol{z}_i + \boldsymbol{K}_{\mathrm{d}i}\boldsymbol{z}_i, \quad (9)$$

where $\boldsymbol{\Lambda}_{\mathrm{z}i}, \boldsymbol{\Lambda}_{\mathrm{x}i}, \boldsymbol{K}_{\mathrm{d}i} \in \mathbb{R}^{n\times n}$ are positive definite diagonal matrices.

3.2 Controller design

The next step consists in designing a tracking controller by using the estimated velocities. Based on (Arteaga-Pérez et al., 2006) we define

$$\boldsymbol{s}_i = \dot{\hat{\boldsymbol{q}}}_i - \boldsymbol{q}_{\mathrm{v}i} + \boldsymbol{\Lambda}_{\mathrm{x}i}\Delta\boldsymbol{q}_i \quad (10)$$

$$\dot{\boldsymbol{\sigma}}_i = \boldsymbol{K}_{\beta i}\boldsymbol{s}_i + \mathrm{sign}(\boldsymbol{s}_i), \quad (11)$$

where $\boldsymbol{K}_{\beta i} \in \mathbb{R}^{n\times n}$ is a positive definite diagonal matrix and $\mathrm{sign}(\boldsymbol{s}_i) = [\mathrm{sign}(s_{i1}), \ldots, \mathrm{sign}(s_{in})]^\top$ with s_{ij} element of $\boldsymbol{s}_i$ for $j = 1, \ldots, n$.

Consider now the following variables

$$\dot{\boldsymbol{q}}_{\mathrm{o}i} = \dot{\hat{\boldsymbol{q}}}_i - \boldsymbol{\Lambda}_{\mathrm{z}i}\boldsymbol{z}_i \quad (12)$$

$$\dot{\boldsymbol{q}}_{\mathrm{r}i} = \boldsymbol{q}_{\mathrm{v}i} - \boldsymbol{\Lambda}_{\mathrm{x}i}\Delta\boldsymbol{q}_i - \boldsymbol{K}_{\gamma i}\boldsymbol{\sigma}_i \quad (13)$$

$$\boldsymbol{s}_{\mathrm{o}i} \stackrel{\triangle}{=} \dot{\boldsymbol{q}}_{\mathrm{o}i} - \dot{\boldsymbol{q}}_{\mathrm{r}i}, \quad (14)$$

where $\boldsymbol{K}_{\gamma i} \in \mathbb{R}^{n\times n}$ is a positive definite diagonal matrix. The proposed control law for the local robot is given by

$$\boldsymbol{\tau}_{\rm l} = -\boldsymbol{K}_{\rm al}\dot{\hat{\boldsymbol{q}}}_{\rm l} - \boldsymbol{K}_{\rm pl}\boldsymbol{s}_{\rm ol}, \quad (15)$$

and for the remote one

$$\boldsymbol{\tau}_{\rm r} = \boldsymbol{K}_{\rm ar}\dot{\hat{\boldsymbol{q}}}_{\rm r} + \boldsymbol{K}_{\rm pr}\boldsymbol{s}_{\rm or}, \quad (16)$$

where $\boldsymbol{K}_{\rm al}, \boldsymbol{K}_{\rm ar}, \boldsymbol{K}_{\rm pr}, \boldsymbol{K}_{\rm pl} \in \mathbb{R}^{n\times n}$ are positive definite diagonal matrices.

3.3 Main result

We claim that, for the bilateral teleoperation system (1)–(2) in closed-loop with the observers (7)–(9) and the control laws (15) and (16), it is always possible to find a proper set of gains so that, if Assumption 1 holds, then

i. Observation errors tend to zero, *i. e.*, $\boldsymbol{z}_i, \dot{\boldsymbol{z}}_i \to \boldsymbol{0}$,
ii. All tracking errors remain bounded,
iii. Whenever $\boldsymbol{\tau}_{\rm h} = \boldsymbol{\tau}_{\rm e} = \boldsymbol{0}$, the system trajectories satisfy
$$\boldsymbol{q}_i(t) \approx \boldsymbol{q}_j(t - T_j(t))$$
i. e., position tracking errors can be made arbitrarily small and if the joint positions tend to a constant value, then all tracking errors tend to zero,
vi. If $\boldsymbol{\tau}_{\rm h} \neq \boldsymbol{0}$ and bounded, the remote robot trajectories satisfy
$$\boldsymbol{q}_{\rm r}(t) \approx \boldsymbol{q}_{\rm l}(t - T_{\rm l}(t)),$$
while the tracking errors on the local manipulator are bounded,
v. If $\boldsymbol{\tau}_{\rm h}$ is not large enough to overcome the input torque $\boldsymbol{\tau}_{\rm l}$ in (15) and $\boldsymbol{\tau}_{\rm e} \neq 0$ and bounded, then the movement of the local robot will tend to be only possible in the direction allowed by the actual constraint on the remote side, *i.e.*, the human operator will have a certain level of telepresence.

Remark 1. Due to space limitations, the proof of our claim is omitted here. However it follows similar steps as in (Arteaga-Pérez et al., 2017). △

Remark 2. Having in Item iii. that $\boldsymbol{q}_i(t) \approx \boldsymbol{q}_j(t - T_j(t))$ and $\boldsymbol{q}_j(t) \approx \boldsymbol{q}_i(t - T_i(t)) \Rightarrow \boldsymbol{q}_i(t) \approx \boldsymbol{q}_i(t - T_j(t) - T_i(t))$, which means that the system trajectories tend either to a periodic signal with period $T_{\rm r}(t) + T_{\rm l}(t)$ or to a constant value, for which it can be exactly guaranteed that $\mathbf{q}_{\rm r} = \mathbf{q}_{\rm l}$, *i. e.*, the consensus problem is solved. This goal can be achieved with the damping provided by the controllers. △

Remark 3. Note that no force sensors are used in our control scheme and that it is not guaranteed that the force the human operator is feeling when trying to move the local manipulator, in the constrained direction, is proportional to that being applied by the remote robot to the actual environment. Furthermore, condition *v.* roughly implies that the human operator will not violate the imposed constrained by pulling too strong. △

4. EXPERIMENT RESULTS

In this section some experimental results are presented for free and constrained motion. The experimental setup is composed of two fully actuated 3-DOF, Geomagic Touch devices. These devices run in different computers in Matlab Simulink (see Fig .1). We implement an ordinary UDP/IP Internet delay to receive and send data. We decided to increase delays artificially by using a normal Gaussian distribution (Salvo-Rossi et al., 2006). The variable time-delays are shown in Figure 2, which plots the sum of both delays.

Fig. 1. Bilateral teleoperation system with two Geomagic Touch

For the control–observer scheme, the following parameters have been chosen:

$\boldsymbol{K}_{{\rm p}i} = {\rm diag}\ \{0.08, 0.09, 0.08\}$,
$\boldsymbol{K}_{{\rm a}i} = {\rm diag}\ \{0.15, 0.1, 0.09\}$,
$\boldsymbol{K}_{\gamma i} = {\rm diag}\ \{0.01, 0.01, 0.01\}$,
$\boldsymbol{\Lambda}_{{\rm x}i} = {\rm diag}\ \{35, 35, 30\}$,
$\boldsymbol{K}_{\beta i} = {\rm diag}\ \{0.000001, 0.000001, 0.000001\}$,
$\boldsymbol{\Lambda}_{{\rm z}i} = \boldsymbol{I}$ and $\boldsymbol{K}_{{\rm d}i} = {\rm diag}\ \{200, 200, 200\}$.

The initial positions are $\boldsymbol{q}_i(0) = \hat{\boldsymbol{q}}_i(0) = [0°, 90°, 90°]^\top$.

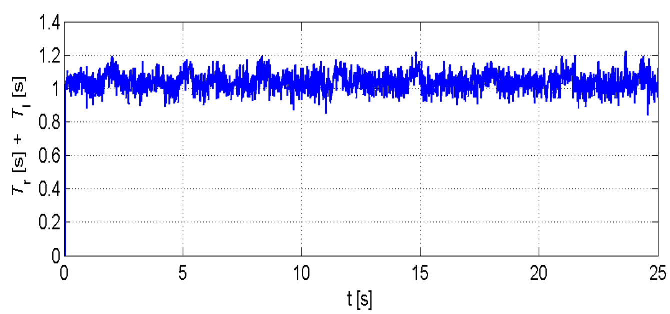

Fig. 2. time-delays $T_{\rm l}(t) + T_{\rm r}(t)$.

4.1 Free motion

In this case, a human operator moves the end-effector of the local manipulator and then drops it, approximately at $t = 11s$; henceforth the systems becomes autonomous. In Figure 3, it can be appreciated how the remote robot is tracking the delayed position of the local robot despite the time variable delays.

In Figure 4, it can be clearly appreciated the effect of the delays and the local robot is not tracking the delayed

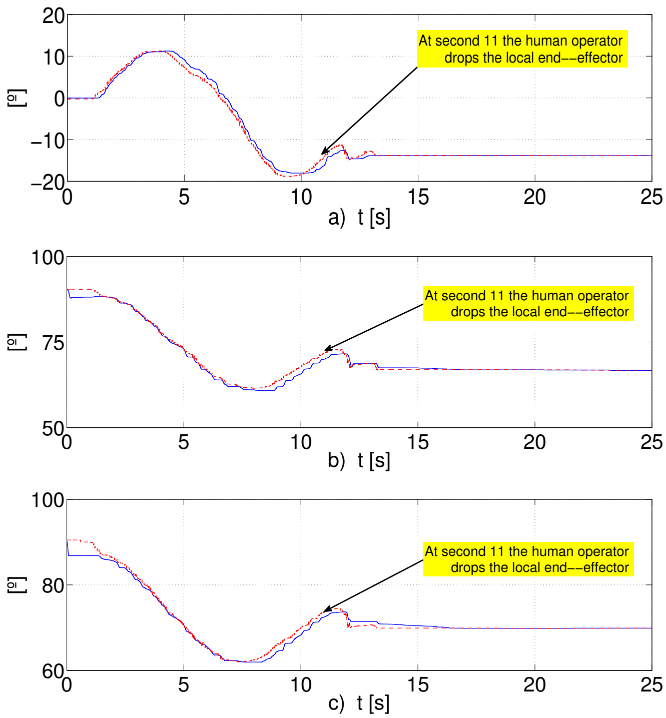

Fig. 3. Free motion. Remote position *vs* delayed local position. a) $q_{r1}(t)$ (——) *vs* $q_{l1}(t - T_l)$ (- - - -) [°]. b) $q_{r2}(t)$ (——) *vs* $q_{l2}(t - T_l)$ (- - - -) [°]. c) $q_{r1}(t)$ (——) *vs* $q_{l1}(t - T_l)$ (- - - -) [°].

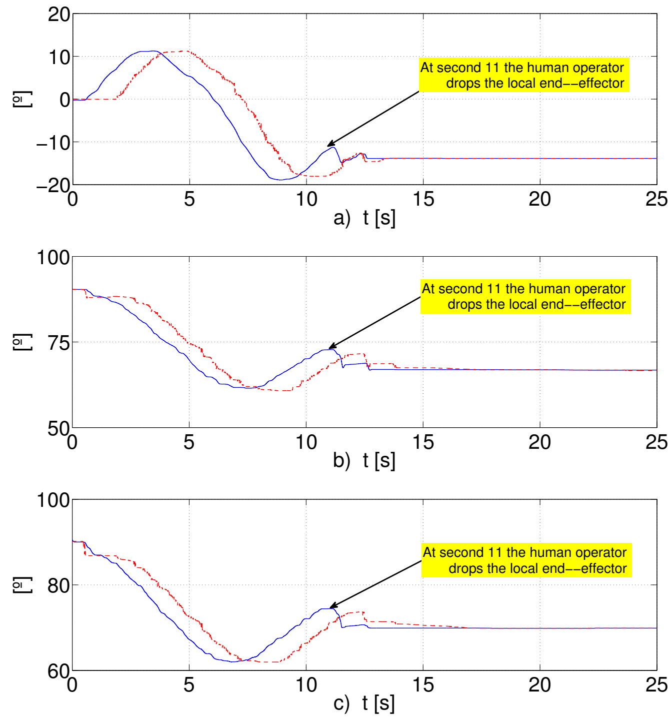

Fig. 4. Free motion. Local position *vs* delayed remote position . a) $q_{l1}(t)$ (——) *vs* $q_{r1}(t - T_r)$ (- - - -) [°]. b) $q_{l2}(t)$ (——) *vs* $q_{r2}(t)$ (- - - -) [°]. c) $q_{l1}(t - T_r)$ (——) *vs* $q_{r1}(t - T_r)$ (- - - -) [°].

remote position. Note that this has been foreseen in the *main result*. However, once the operator drops the end-effector of the local manipulator position tracking is established. This fact can be appreciated in Figure 5, where the tracking errors are shown to converge to zero.

Figure 6 depicts the observation errors. Note that these errors are bounded and tend to be nearly zero from the beginning. The errors seem to be not affected by the delays. Further, in theory, one can arbitrarily increase the observer gains and thus arbitrarily reduce the observation errors, however performance might be downgraded.

4.2 Constrained Motion

For this case, as shown in Figure 1, a stiff box is located in the remote environment. Here the human operator moves down the local robot in order for the remote robot to become in contact with such box. In any case the human operator releases the local robot end effector. In Figure 7 it can be seen that the remote robot is also tracking the delayed position of the local robot. Figure 8 shows the position of local robot *vs* the delayed position of the remote manipulator, where it is possible to see the effect of the delays. In both cases the remote robot tracks the local position.

Figure 9 shows the position tracking errors, which are bounded as foreseen in the *main result*. Moreover, in Figure 10 one can see that the observation errors are not affected by the delays and they tend to zero when position tracking is established. Note that the observation error also shows good performance as in the free motion case.

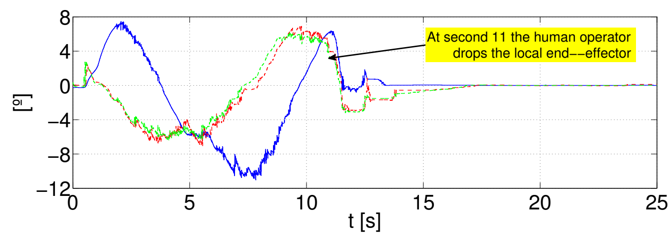

(a) $\Delta \boldsymbol{q}_{l1}$(——), $\Delta \boldsymbol{q}_{l2}$(- - -), $\Delta \boldsymbol{q}_{l3}$(- - -)

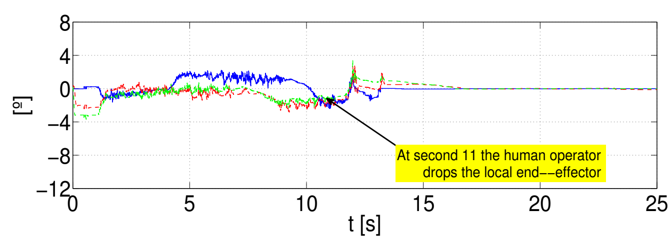

(b) $\Delta \boldsymbol{q}_{r1}$(——), $\Delta \boldsymbol{q}_{r2}$ (- - -), $\Delta \boldsymbol{q}_{r3}$(- - -)

Fig. 5. Free motion. Position tracking errors.

Finally, when the remote manipulator gets in touch with the box, the end-effector movement is stopped and the person can feel it since also the local robot cannot move in that direction. Then, the operator has a certain feeling of telepresence. Figure 11 depicts the surface reconstruction by the local manipulator.

5. CONCLUSIONS

In this work, a controller that does not make use of velocity measurements for robot teleoperation systems is

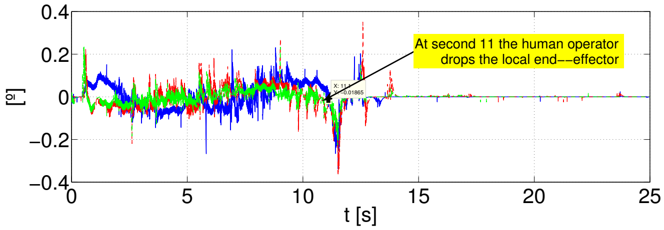

(a) $\boldsymbol{z}_{\mathrm{l}1}$ (——), $\boldsymbol{z}_{\mathrm{l}2}$ (- - -), $\boldsymbol{z}_{\mathrm{l}3}$ (- - -)

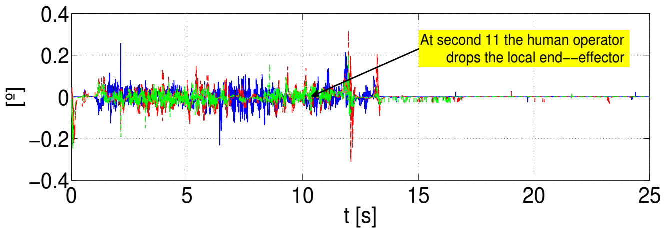

(b) $\boldsymbol{z}_{\mathrm{r}1}$ (——), $\boldsymbol{z}_{\mathrm{r}2}$ (- - -), $\boldsymbol{z}_{\mathrm{r}3}$ (- - -)

Fig. 6. Free motion. Observation errors.

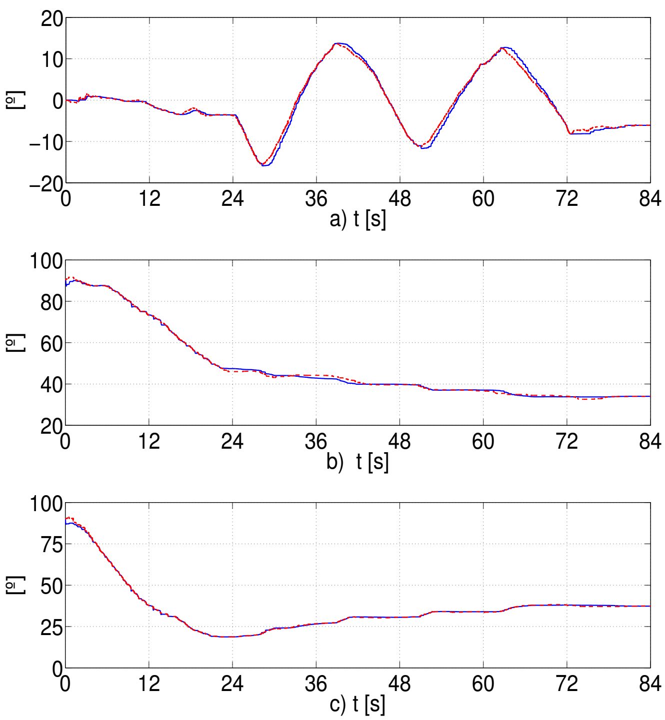

Fig. 7. Constrained motion. Remote position *vs* delayed local position. a) $q_{\mathrm{r}1}(t)$ (——) *vs* $q_{\mathrm{l}1}(t - T_{\mathrm{l}})$ (- - - -) [°]. b) $q_{\mathrm{r}2}(t)$ (——) *vs* $q_{\mathrm{l}2}(t - T_{\mathrm{l}})$ (- - - -) [°]. c) $q_{\mathrm{r}1}(t)$ (——) *vs* $q_{\mathrm{l}1}(t - T_{\mathrm{l}})$ (- - - -) [°].

introduced with the following properties. In free motion, without a human operator, the bilateral scheme is aimed at making the manipulators tracking their positions until they reach a consensus point. Further, if the human operator moves either the local or remote manipulator, the other robot will track it is trajectory with the corresponding delay up to an ultimately arbitrarily small final bound of the error. Moreover, in constrained motion the human operator has a certain degree of telepresence. We assume that the communications might induce bounded variable time-delays. The observation errors are observed to converge to zero.

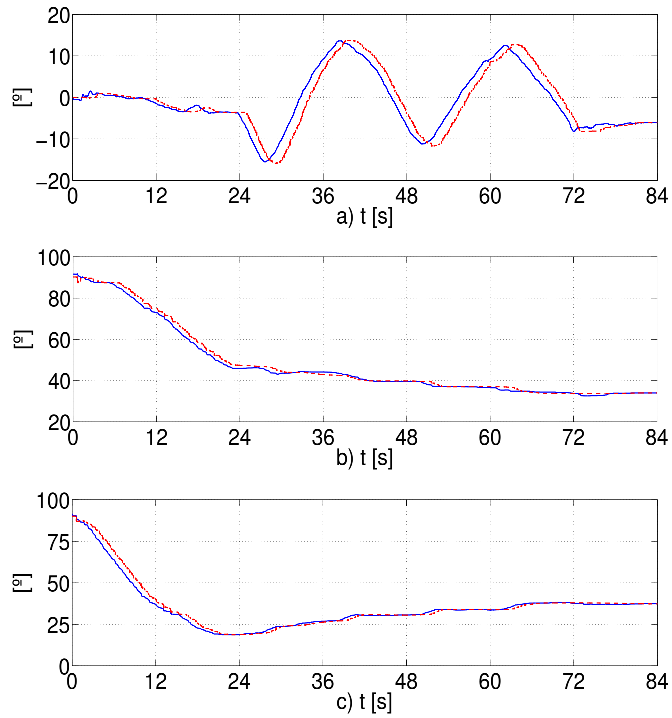

Fig. 8. Constrained motion. Local position *vs* delayed remote position. a) $q_{\mathrm{l}1}(t)$ (——) *vs* $q_{\mathrm{r}1}(t - T_{\mathrm{r}})$ (- - - -) [°]. b) $q_{\mathrm{l}2}(t)$ (——) *vs* $q_{\mathrm{r}2}(t)$ (- - - -) [°]. c) $q_{\mathrm{l}1}(t - T_{\mathrm{r}})$ (——) *vs* $q_{\mathrm{r}1}(t - T_{\mathrm{r}})$ (- - - -) [°].

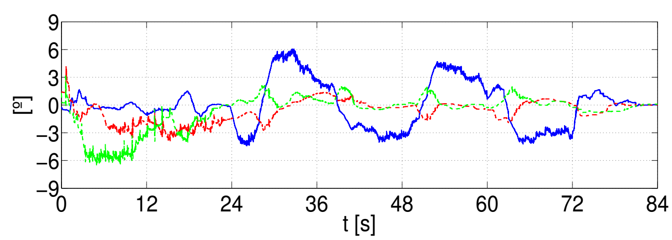

(a) $\Delta\boldsymbol{q}_{\mathrm{l}1}$(——), $\Delta\boldsymbol{q}_{\mathrm{l}2}$(- - -), $\Delta\boldsymbol{q}_{\mathrm{l}3}$(- - -)

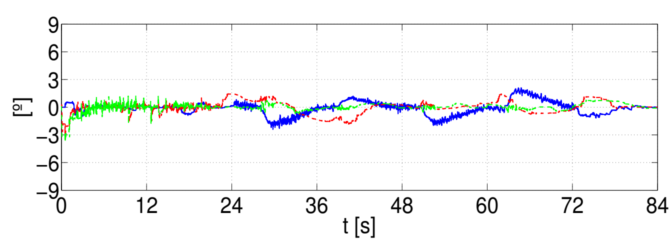

(b) $\Delta\boldsymbol{q}_{\mathrm{r}1}$(——), $\Delta\boldsymbol{q}_{\mathrm{r}2}$ (- - -), $\Delta\boldsymbol{q}_{\mathrm{r}3}$(- - -)

Fig. 9. Constrained motion. Tracking errors.

Two experiments have been implemented to test the proposed algorithm. The first is for free movement, where the operator moves the local end-effector and then he/she releases it. After such moment, the teleoperation system becomes autonomous and position errors are shown to converge to zero. The second experiment is for constrained movement, where the remote robot interacts with a rigid object. It is shown that the motion of the local robot becomes also constrained, giving the operator the feeling of telepresence.

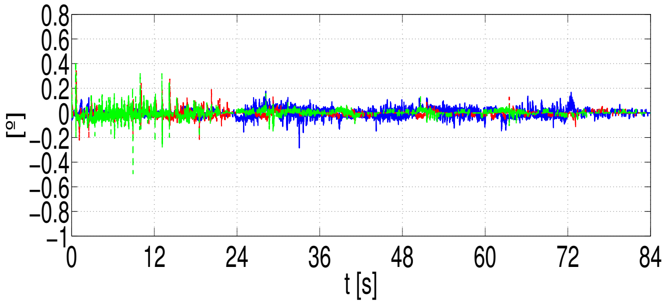

(a) $\boldsymbol{z}_{l1}$ (——), $\boldsymbol{z}_{l2}$ (- - -), $\boldsymbol{z}_{l3}$ (- - -)

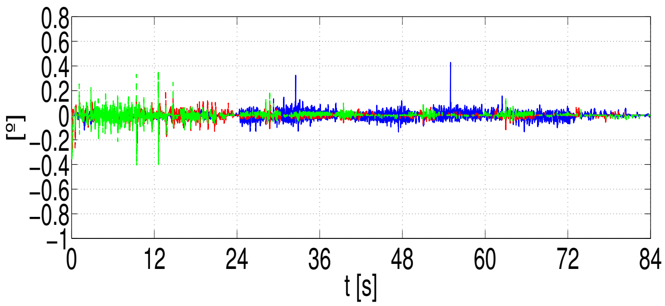

(b) $\boldsymbol{z}_{r1}$ (——), $\boldsymbol{z}_{r2}$ (- - -), $\boldsymbol{z}_{r3}$ (- - -)

Fig. 10. Constrained motion. Observation errors.

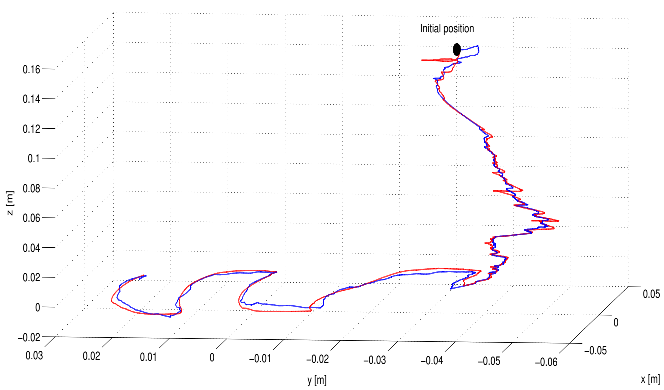

Fig. 11. Constrained motion. Surface reconstruction (local) (——) *vs* actual (remote) (- - -)[m].

ACKNOWLEDGEMENTS

This work is supported by the **DGAPA-UNAM** under grant **IN114617**.

REFERENCES

Aldana, C.I., Romero, E., Nuño, E., and Basañez, L. (2015). Pose consensus in networks of heterogeneous robots with variable time delays. *International Journal of Robust and Nonlinear Control*, 25(14), 2279–2298.

Arteaga-Pérez, M.A., Castillo-Sánchez, A.M., and Parra-Vega, V. (2006). Cartesian control of robots without dynamic model and observer design. *Automatica*, 42, 473–480.

Arteaga-Pérez, M.A., Morales, M., López, M., and Nuño, E. (2016). Observer based bilateral teleoperation for delayed systems: New proposal and experimental results. In *Proc. of the 42nd IEEE Industrial Electronics Conference (IEEE IECON2016)*. Florence. Italy.

Arteaga-Pérez, M., López-Recillas, L., López, M., and Nuño, E. (2017). Observer design for bilateral teleoperation systems with variable time delays. In *Proceedings of IFAC World Congress*. Toulouse, France.

Astolfi, A., Ortega, R., and Venkatraman, A. (2010). A globally exponentially convergent immersion and invariance speed observer for mechanical systems with non-holonomic constraints. *Automatica*, 46(1), 182–189.

Chopra, N., Spong, M.W., and Lozano, R. (2008). Synchronization of bilateral teleoperators with time delay. *Automatica*, 44, 2142–2148.

Hokayem, P. and Spong, M. (2006). Bilateral teleoperation: an historical survey. *Automatica*, 42(12), 2035–2057.

Kelly, R., Santibáñez, V., and Loria, A. (2005). *Control of robot manipulators in joint space*. Advanced textbooks in control and signal processing. Springer–Verlag.

Nuño, E., Basañez, L., Ortega, R., and Spong, M.W. (2009). Position tracking for non–linear teleoperators with variable time delay. *International Journal of Robotics Research*, 28(7), 895–910.

Nuño, E., Ortega, R., Barabanov, N., and Basañez, L. (2008). A globally stable PD controller for bilateral teleoperators. *IEEE Transactions on Robotics*, 24(3), 753–758.

Nuño, E., Basañez, L., and Ortega, R. (2011). Passivity-based control for bilateral teleoperation: A tutorial. *Automatica*, 47(3), 485–495.

Nuño, E. and Ortega, R. (2017). Achieving consensus of euler-lagrange agents with interconnecting delays and without velocity measurements via passivity-based control. *IEEE Transactions on Control Systems Technology. DOI:10.1109/TCST.2017.2661822*, 1–11.

Passenberg, C., Peer, A., and Buss, M. (2010). A survey of environment-, operator-, and task-adapted controllers for teleoperation systems. *Mechatronics*, 20, 787–801.

Salvo-Rossi, P., Romano, G., Palmieri, F., and Iannello, G. (2006). Joint end–toend loss–delay hidden Markov model for periodic UDP traffic over the Internet. *IEEE Transactions on Signal Processing*, 54(2), 530–541.

Sarras, I., Nuño, E., Basañez, L., and Kinnaert, M. (2016). Position tracking in delayed bilateral teleoperators without velocity measurements. *International Journal of Robust and Nonlinear Control*, 26(7), 1437–1455.

Sarras, I., Nuño, E., and Basañez, L. (2014). An adaptive controller for nonlinear teleopertors with variable time-delays. *Journal of the Franklin Institute*, 351(10), 4817–4837.